GA23 / P35

Structure determination of Sn on Cu(111) using LEED

Rezwan Ahmed, Takeshi Nakagawa, Seigi Mizuno
Department of Molecular and Material Sciences, Kyushu University, Kasuga, Kasugakoen, 6-1, Fukuoka 816-8580, Japan
Email: r_ahmed17@yahoo.com

Abstract: *The 2D hexagonal structure of tin atoms which is termed stanene is structurally determined on a Cu(111) substrate using low energy electron diffraction. The structural analysis of Cu{111}-p(2x2)-Sn at a coverage of 0.5 at low temperature reveals the relaxation of underlying Cu atoms, which stabilizes the formation of almost zero-buckled Sn atoms forming a honeycomb structure. Our result using quantitative low energy electron diffraction conclusively reveals an ultra-flat stanene structure that complements well with the previous calculations. The detailed structural analysis presented in this article is expected to give in-depth information for characterizing the properties of as-grown stanene.*

Keywords: Stanene; Cu(111); LEED

1. INTRODUCTION

The two dimensional (2D) group IVA materials of carbon, silicon, germanium, tin and lead which are termed as graphene, silicene, germanene, stanene and plumbene respectively having single layer of atoms organized in a honeycomb like lattice possesses striking physical properties due to its unique structure. [1]–[3] All these materials are predicted to exhibit band gap due to spin orbit coupling which makes them 2D topological insulators. [4]–[9] Graphene has been extensively studied in the past for its relative ease of fabrication however, in the last few years experimental studies of other 2D materials as we move down the same group have taken the limelight due to the stronger spin-orbit coupling which results in additional intriguing properties in the field of solid state physics. [9]- [12] Among them, stanene is considered to be highly promising 2D material due to its exclusive enriched properties such as topological superconductivity, near-room temperature quantum anomalous Hall (QAH) effect, giant magnetoresistance and enhanced thermoelectricity. [7]-[8], [11]-[13][14] The successful growth and realization of 2D materials largely depend on the perfect selection of underlying substrates, as proper interaction between substrate and 2D material is necessary. The growth of stanene was elusive until in recent years there are several reports of successful fabrication of stanene in different substrates which have gradually led to the realization of many of these interesting properties.

One of the first experimental realization of the theoretically predicted stanene was reported by Zhu et al. where the 2D material was grown on Bi2Te3 using molecular beam epitaxy and adopts Vollmer-Weber (island) growth mode. [15] Later on, stanene was further successfully reported on substrates like Sb(111), InSb(111), Bi(111), Au(111), Ag(111) and PbTe(111). [16][17][18][19][20][21] Besides grown on diverse substrates, the other distinct structural features of as grown stanene for each of these cases is the difference of buckling between the Sn atoms. The DFT calculations suggest that stanene becomes more stable as the buckling is reduced. [9][22][23].

The study of ultrathin Sn films on Cu(111) substrate is well studied which generally forms a surface alloy at or above room temperature due to the high solubility of Sn on Cu. [24][25] The realization of 2D tin atoms on Cu(111) substrate at low temperature was first addressed by Xihui et al. proposing one atom per unit cell of p(2x2) structure. [26] However, recently Deng et al have observed the epitaxial growth of stanene on Cu(111) having honeycomb structure and an unusually ultra-flat zero-buckling geometry using STM and supported by DFT calculations.[27] This suggests the importance of underlying interaction of substrates with stanene in stabilizing the ultra-flat 2D structure. However, the interaction and relaxation of the underlying substrate is not investigated in previous reports which can be an important factor in understanding the overlayer structure with zero buckling nature.

In this report we have investigated the structural parameters of stanene on Cu(111) more distinctively using quantitative tensor low energy electron diffraction which is sensitive to the surface and provides detailed structural parameters compared to STM alone. [25]-[26] Because the substrate plays an important role is stabilizing the zero-buckling stanene structure, we tried to investigate the role of relaxation of first few layers of Cu atoms and the bonding between the adsorbed Sn atoms at both fcc and hcp site with that of the underlying Cu atoms. This detailed structural analysis can pave a way for understanding the interactions of Cu with the Sn atoms arranged in honeycomb structure and hence can help for further characterizing the properties of as grown stanene.

2. Experimental Procedure

The experiments were performed in an ultra-high vacuum chamber with a base pressure of 5 x 10-8 Pa, which is equipped with four grid LEED system including in situ sample preparation and adsorbate (Sn) deposition. At first the Cu(111) substrate was cleaned with several cycles of Ar+ ion sputtering (1 kV, 7 μA, 15 min) and subsequent annealing at 800 K until a sharp (1x1) LEED pattern was recorded. The sample was pre-cooled with liquid N2 until the temperature reaches ~150 K before the Sn was evaporated by thermal heating from a tantalum tube onto the sample. The deposition is sequentially monitored until p(2x2) structure is obtained in the LEED pattern. The sample was further cooled until 130 K with liquid N2 when the p(2x2) structure is sharped which

were observed using a digital charge-coupled device camera with computer-controlled data acquisition system. [30] The intensity for nine inequivalent spots of Sn-p(2x2)-Cu(111) structure having three fold rotational symmetry is recorded for an energy range of 70-450 eV. The Barbieri/Van Hove symmetrized automated tensor LEED package was used to calculate the theoretical I(E) curves of the structure models to determine the atomic positions. [31] The calculations for the atomic scattering was performed by considering 13 phase shifts (lmax = 12) whereas the imaginary part of the inner potential (Voi) was fixed to −5.0 eV and the real part was determined through theoretical-experimental matching and attributed by minimizing Pendry's reliability factor (Rp). [32] The error bars on the structural parameters were calculated from the variance of Rp, $\Delta R = Rmin(8|Voi|/\Delta E)1/2$, where Rmin is the minimum Rp value and ΔE is the total energy range of the experimental I(E) curves. [32]

3. Results and Discussion

In order to determine the structural model of p(2x2)-Sn we have analyzed ten structures. All the structural models represent p3m1 symmetry. Each of the structures are optimized however, the first model having honeycomb structure indicates the lowest RP factor which was also proposed by Deng et al. [27] Further optimization of the Debye temperatures of Sn, Cu, and structural parameters led to more reduced RP factor of 0.14 for model 1. The detailed structural parameters for the model 1 with top and cross sectional views after optimization is shown in Fig. 1 with Debye temperatures of Sn, first layer Cu, second layer Cu, third layer Cu and operating temperature of 90, 230, 250, 300 and 150 K respectively. The comparison between the calculated I(E) curves of the best fit model with the experimental curves is shown in Fig. 2 which represents total energy range of

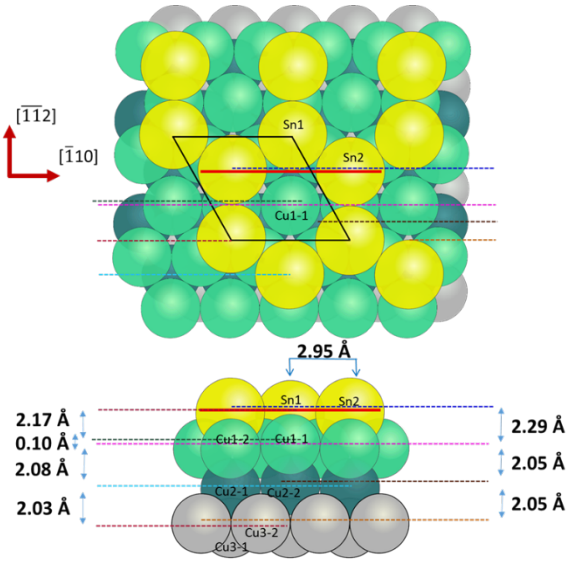

Fig. 1 Top and cross sectional views of the optimized honeycomb stanene structure Cu(111)-p(2x2) (Model 1 in Fig. 1). Atomic size ratios between the Cu and Sn atoms are roughly reflected. Sn1 indicates Sn atom in the fcc hollow site, Sn2 indicates Sn atom in hcp hollow site. There are four Cu atoms in the unit cell. Cu1-1 and Cu1-2 notations indicate first layer Cu and their corresponding number. The same is true for the second and third layer Cu atoms.

1670 eV having 9 symmetrically inequivalent beams. The numerical parameters of the lateral displacement and corresponding vertical displacement of the Sn and underneath Cu atoms alongside the error ranges are listed in Table 1. All the lateral displacements were measured relative to the ideal three-fold hollow sites while the vertical displacement is calculated relative to the ideal first layer Cu atoms.

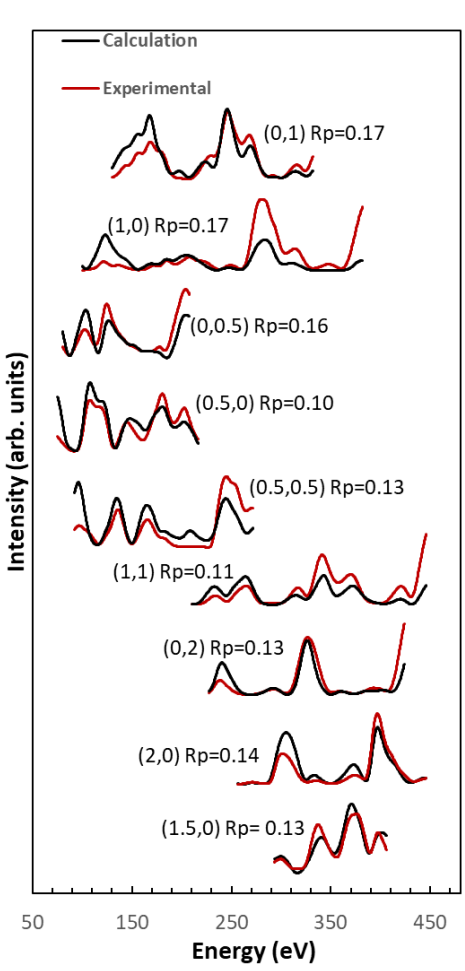

Fig. 2 Comparison between the experimental (red line) and best fit calculated (black line) LEED I(E) spectra for Cu(111)-p(2x2)-Sn structure.

The coverage of the optimized honeycomb structure is 0.5 in a unit cell with one Sn atom in the face-centered cubic hollow site while the other in the hexagonal close-packed hollow site denoted as Sn1 and Sn2 respectively from hereon. In the previous study with STM, Deng et al. showed no buckling in the stanene with two Sn atoms having the same apparent height of 1.8 Å relative from the first Cu layer. [27] It is quite interesting as the Sn atoms are positioned in two different sites so they are expected to have different interactions with surrounding Cu atoms which would result in different adsorption heights for optimizing the energy. The height between the two Sn atoms in our optimized calculation shows 0.02 Å however, the difference is smaller than the error range which dismiss this difference into consideration.

One common structural phenomenon observed from all the calculations that led to the optimized structure is that the Sn1 which is in the FCC position has always dipped to the Cu surface more compared to the Sn2 in

HCP site. On contrary, interestingly the average bond length of Sn1 is longer than the Sn2 with corresponding first layer Cu atoms as shown in Table 2. To interpret the situation, we analyzed the structural parameters and found that this is due to the lateral displacement of the Cu atoms relative to their positions which is numerically

Table 1 Structural parameters for the optimized best fit structure for p(2x2)-Sn structure. Atoms and their numbers are referenced in Fig. 2. The height is calculated from the starting position of first Cu layer where 0 indicates no displacement of atoms in the specified direction due to symmetry requirement.

Atom	Lateral displacement (Å)		Height (Å)
Sn1	0	0	-2.23±0.06
Sn2	0	0	-2.25±0.05
Cu1-1	0	0	-0.06±0.02
Cu1-2	0	0.06±0.08	0.04±0.02
Cu1-3	0.06±0.08	-0.03±0.08	0.04±0.02
Cu1-4	-0.06±0.08	-0.03±0.08	0.04±0.02
Cu2-1	0	0	2.12±0.02
Cu2-2	0	-0.01±0.09	2.09±0.02
Cu2-3	0.01±0.09	0.01±0.09	2.09±0.02
Cu2-4	-0.01±0.09	0.01±0.09	2.09±0.02
Cu3-1	0	0	4.14±0.05
Cu3-2	0	0.03±0.13	4.15±0.05
Cu3-3	0.03±0.13	-0.02±0.13	4.15±0.05
Cu3-4	-0.03±0.13	-0.02±0.13	4.15±0.05

presented in Table 1. The lateral and vertical displacement of the first layer Cu atoms also have an impact on the subsequent underneath Cu layers as can be seen from the Table 1. Similar to the first layer Cu atoms the second layer Cu atoms also have a lateral and vertical relaxation to stabilize the structure which is carried forward to the third Cu layer as well.

The bond length between the Sn atoms in our LEED calculation is 2.95 Å which is comparable to the bulk α-

Bond	p(2x2)-Sn
Sn1-Cu1-2,3,4	2.75
Sn2-Cu1-1,2,3	2.69
Cu1-1-Cu1-1,2,3	2.56

Sn and freestanding stanene which also complements well with the previous study. [9][27] The height between the Sn and the first layer Cu atoms is 2.17 ± 0.28 Å which complements well with the theoretical adsorption height of stanene on Cu(111) but is little higher than the STM line profile of 1.8 Å. However, the average bond length between the Sn1 and the first layer Cu atoms is 2.75 Å which is comparable with the bulk Sn-Cu bond of 2.73 Å. Therefore, we can deduce that our average calculated height between the Sn and first layer Cu atoms is reasonable.

We also determined the overall relaxation in [111] direction of the Sn adsorbed Cu(111) surface with respect to clean Cu(111) surface to understand the contribution of the substrate relaxation in stabilizing the flat stanene structure. The interlayer distance between the first and second Cu layer is 2.08 Å whereas it is 2.05 Å between the second and third layers compared to the bulk value of 2.08 Å. [33] It is quite apparent that instead of compression between the first two layers with respect to the interlayer distance between the second and third layer which is present in clean Cu(111), the adsorption of Sn as an overlayer has an opposite effect on Cu(111) surface. This is due to the fact that Cu1-1 atom has vertically translated upward by 0.06 Å to neutralize the lateral displacement of the other Cu atoms in first layer which in turn optimized the buckling effect between the two Sn atoms. Therefore, from the above discussion it is clearly evident that the underlying Cu atoms provoke the formation of ultra-flat stanene by subsidizing the overall relaxation on the surface. These detail numerical data of the structure obtained using experimental QLEED analysis is expected to provide important information for the characterization of the properties of stanene as well as understanding the role of substrate in stabilizing other 2D materials.

4. REFERENCES

[1] V. M. Apalkov and T. Chakraborty, "Tunability of the fractional quantum Hall states in buckled Dirac materials," Phys. Rev. B - Condens. Matter Mater. Phys., vol. 90, no. 24, pp. 1–6, 2014.

[2] H. Wu and F. Li, "First-Principles Calculation on Geometric, Electronic and Optical Properties of Fully Fluorinated Stanene: a Large-Gap Quantum Spin Hall Insulator," Chinese Phys. Lett., vol. 33, no. 6, p. 67101, Jun. 2016.

[3] T. Taniguchi et al., "Observation of the quantum spin Hall effect up to 100 kelvin in a monolayer crystal," Science (80-.)., vol. 79, no. January, pp. 76–79, 2018.

[4] S. Sadeddine et al., "Compelling experimental evidence of a Dirac cone in the electronic structure of a 2D Silicon layer," Sci. Rep., vol. 7, pp. 1–7, 2017.

[5] M. E. Dávila, L. Xian, S. Cahangirov, A. Rubio, and G. Le Lay, "Germanene: A novel two-dimensional germanium allotrope akin to graphene and silicene," New J. Phys., vol. 16, 2014.

[6] J. Gao, G. Zhang, and Y. W. Zhang, "Exploring Ag(111) substrate for epitaxially growing monolayer stanene: A first-principles study," Sci. Rep., vol. 6, no. April, pp. 1–8, 2016.

[7] Y. Fang et al., "Quantum spin hall states in stanene/Ge(111)," Sci. Rep., vol. 5, no. 111, pp. 1–8, 2015.

[8] J. Wang, Y. Xu, and S. C. Zhang, "Two-dimensional time-reversal-invariant topological superconductivity in a doped quantum spin-Hall insulator," Phys. Rev. B - Condens. Matter Mater. Phys., vol. 90, no. 5, pp. 1–5, 2014.

[9] Y. Xu et al., "Large-gap quantum spin hall insulators in tin films," Phys. Rev. Lett., vol. 111, no. 13, pp. 1–5, 2013.

[10] Y. Xu, Z. Gan, and S. C. Zhang, "Enhanced thermoelectric performance and anomalous seebeck

effects in topological insulators," Phys. Rev. Lett., vol. 112, no. 22, pp. 1–5, 2014.
[11] A. Molle, J. Goldberger, M. Houssa, Y. Xu, S. C. Zhang, and D. Akinwande, "Buckled two-dimensional Xene sheets," Nat. Mater., vol. 16, no. 2, pp. 163–169, 2017.
[12] S. Rachel and M. Ezawa, "Giant magnetoresistance and perfect spin filter in silicene, germanene, and stanene," Phys. Rev. B - Condens. Matter Mater. Phys., vol. 89, no. 19, pp. 1–6, 2014.
[13] M. Liao et al., "Superconductivity in few-layer stanene," Nat. Phys., vol. 14, no. 4, pp. 344–348, 2018.
[14] S. Nigam, S. Gupta, D. Banyai, R. Pandey, and C. Majumder, "Evidence of a graphene-like Sn-sheet on a Au(111) substrate: Electronic structure and transport properties from first principles calculations," Phys. Chem. Chem. Phys., vol. 17, no. 10, pp. 6705–6712, 2015.
[15] F. F. Zhu et al., "Epitaxial growth of two-dimensional stanene," Nat. Mater., vol. 14, no. 10, pp. 1020–1025, 2015.
[16] C. Z. Xu et al., "Gapped electronic structure of epitaxial stanene on InSb(111)," Phys. Rev. B, vol. 97, no. 3, pp. 1–5, 2018.
[17] J. Yuhara et al., "Large area planar stanene epitaxially grown on Ag(1 1 1)," 2D Mater., vol. 5, no. 2, 2018.
[18] Y. Zang et al., "Realizing an Epitaxial Decorated Stanene with an Insulating Bandgap," Adv. Funct. Mater., vol. 28, no. 35, pp. 1–7, 2018.
[19] J. Gou et al., "Strain-induced band engineering in monolayer stanene on Sb(111)," Phys. Rev. Mater., vol. 1, no. 5, pp. 1–6, 2017.
[20] M. Maniraj et al., "A case study for the formation of stanene on a metal surface," Commun. Phys., vol. 2, no. 1, pp. 1–9, 2019.
[21] Y.-H. Song et al., "High-buckled R3 stanene with topologically nontrivial energy gap," arXiv:1707.08657 [cond-mat.mtrl-sci], 2017.
[22] S. R. Song, J. H. Yang, S. X. Du, H. J. Gao, and B. I. Yakobson, "Dirac states from px,y orbitals in the buckled honeycomb structures: A tight-binding model and first-principles combined study," Chinese Phys. B, vol. 27, no. 8, 2018.
[23] A. Molle, J. Goldberger, M. Houssa, Y. Xu, S. C. Zhang, and D. Akinwande, "Buckled two-dimensional Xene sheets," Nat. Mater., vol. 16, no. 2, pp. 163–169, 2017.
[24] J. F. Aguilar, R. Ravelo, and M. I. Baskes, "Morphology and dynamics of 2D Sn-Cu alloys on (100) and (111) Cu surfaces," Model. Simul. Mater. Sci. Eng., vol. 8, no. 3, pp. 335–344, 2000.
[25] S. H. Overbury and Y. S. Ku, "Formation of stable, two-dimensional alloy-surface phases: Sn on Cu(111), Ni(111), and Pt(111)," Physical Review B, vol. 46, no. 12. pp. 7868–7872, 1992.
[26] X. Liang, J. H. Deng, L. J. Fan, Y. W. Yang, and D. A. Luh, "Nonalloying surface reconstructions of ultrathin Sn films on Cu(111) investigated with LEED, XPS, and photoelectron extended fine structure analysis," Phys. Rev. B - Condens. Matter Mater. Phys., vol. 84, no. 7, pp. 1–6, 2011.
[27] J. Deng et al., "Epitaxial growth of ultraflat stanene with topological band inversion," Nat. Mater., vol. 17, no. 12, pp. 1081–1086, 2018.
[28] M. A. VANHOVE J CERDA P SAUTET M.-L BOCQUET M SALMERON, "Surface structure determination," Vacuum, vol. 31, no. 10–12, pp. 399–405, 1981.
[29] K. Heinz and L. Hammer, "Combined application of LEED and STM in surface crystallography," J. Phys. Chem. B, vol. 108, no. 38, pp. 14579–14584, 2004.
[30] S. Mizuno, H. Tochihara, A. Barbieri, and M. A. Van Hove, " Completion of the structural determination of and rationalization of the surface-structure sequence (2×1)→(3×3)→(4×4) formed on Cu(001) with increasing Li coverage," Phys. Rev. B, vol. 52, no. 16, pp. 658–662, 1995.
[31] M. A. Van Hove et al., "Automated determination of complex surface structures by LEED," Surf. Sci. Rep., vol. 19, no. 3–6, pp. 191–229, 1993.
[32] J. B. Pendry, "Reliability factors for {LEED} calculations," J. Phys. C Solid State Phys., vol. 13, no. 5, pp. 937–944, Feb. 1980.
[33] S. Review, W. F. Chung, and Q. Cai, "Cu (111) Surface Relaxation by Vleed," no. August, 1995.